Determination of the Operational Parameters of a Planar Robot with Three Joints

Muharrem Zeytinoğlu mzeytin@uludag.edu.tr
Department of Biosystems Engineering
Faculty of Agriculture
Uludağ University
Bursa, 16059, Turkey

Halil Ünal hunal@uludag.edu.tr
Department of Biosystems Engineering
Faculty of Agriculture
Uludağ University
Bursa, 16059, Turkey

Abstract

Robots are currently made in numerous types and are used in diverse roles such as production lines, daily living activities and some security fields. These types of robots are well designed and successfully applied in many areas requiring high sensitivity and stability. The aim of this study was to determine the optimum values of several operational parameters for a planar robot with respect to robot design and construction. With this aim, a small planar robot with a three-jointed arm activated by hydraulic cylinders in each segment was evaluated using a technical design drawing. The arm motions of the planar robot are rotary and parallel within a vertical plane. The resulting optimal operational parameters of the planar robot were determined as starting and target positions of 31.5 cm and 55 cm, respectively, on the x-axis and 17.18 cm and 118.44 cm on the y–axis. Time-position and time-velocity graphs were constructed corresponding to the orbit-planning parameters, resulting in Cartesian velocities for the terminal processor of 13.98 m/sec on the x-axis and 20.16 m/sec on the y-axis at 1.5 seconds after initiation. The maximum power consumption of the robot was determined as 1 kW according to the outer load and arm weights.

Keywords: Planar robot, Orbit-planning parameter, Cartesian velocity, Kinematic analysis.

1. INTRODUCTION

Planar robots are well recognized as practical robots; they are generally of linear construction and operate on a fixed route in a process implemented by rotating or sliding in parallel to a given plane. These types of robots have mostly been applied to linear activities such as the rapid lifting, carrying, and placement of various parts [4]. The vibrational rate of planar robots is lower than for other kinds of more versatile robots because planar robots are required to perform fewer operations; therefore, planar robots have an important advantage with respect to sensitivity and stability.

Currently, a number of different types of planar robots are required in industrial, agricultural, and security areas as well as daily living activities; they are constructed in a diversity of designs and dimensions for these different applications [9]. In this study, a planar robot was designed from a technical drawing (Figure 1) with three arm segments and three joints. Each segment is moved by a hydraulic cylinder; the motion of the arm segments is in parallel to a

plane, and the entire arm rotates. The planar robot also has a terminal processor, i.e., a hook attached to its end point, which moves linearly and rotates in the same plane between the starting point, which is at the inactive position of the hydraulic cylinders, and the target point, which is at the fully actuated position of the hydraulic cylinders. The inverse analysis can be made by considering the planar robot to work in the opposite direction, i.e., by swapping the starting and target points. The planar robot was designed to lift a specific load. The operational parameters investigated were the starting and target positions, the time-position and time-velocity relations, the Cartesian velocities of the terminal processor and the maximum power consumption of the robot, which in turn depend on the robot design parameters. The optimal operational parameters were determined by means of several analytical methods; to this end, time-position and time-velocity graphs were constructed from the results of a kinematic analysis of the robot [5]. The motion of the terminal processor was the main factor in the kinematic analysis, and its motion is determined by the configuration of the joint points in the action plane. The motion can be configured into various paths, such as a linear, circular, sinusoidal or irregular path [1]. Kinematic analysis was performed by orbit planning, which is necessary to ensure that robot motion is steady and controllable, without vibration or deflection from the working space [3].

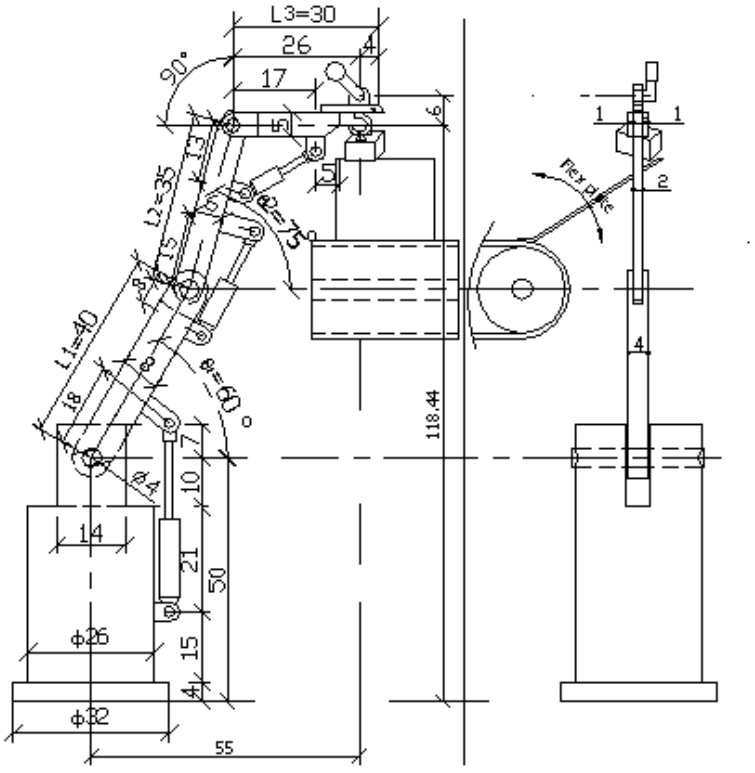

FIGURE 1: Views of the planar robot with three joints in the target position; all dimensions are in cm

Orbit planning for robots can be done using either of two methods: the Cartesian and joint-space methods. In this study, the joint-space method was used; here, each joint was considered to be independent of the others, and therefore, the velocity of each joint was different in the orbit planning. In this model, the hydraulic-cylinder pressures and capacities are also different when reaching the required position of the terminal processor. A detailed view of the orbit planning was obtained through a third-degree polynomial equation, and the time-position and time-velocity relations were determined from the solutions of the polynomial equation 5. Determining the Cartesian velocities from the operational parameters of the robot is very important with respect to the level of swing inertia encountered during the lifting of a specific load. The working velocity and arm-segment lengths of the robot are the determining factors of the Cartesian velocities. The maximum robot power consumption was calculated

corresponding to the planar velocities of the solid materials [6]. The final results for the optimum operational parameters are given in Table 3.

As shown in Figure 1, the robot under study has a base frame constructed of thick-walled steel tubing that is located on the floor at one side. The terminal processor has a top working weight combined with a hook; these are restrained by a stop in the starting position of the lifting operation. As the lifting operation concludes, the hook is cleared on the reverse side by the balanced movement of the top weight, facilitating the release of the load from the hook, thus leaving the load on the conveyor band in the target position. The hook is located at the end of the third arm segment, and its weight is considered as equal to the empty volume of the third arm segment. The hook-lifted load is 40 N, and this weight was added to the weight of arm Segment 3 in the calculation of the robot's power consumption.

2. DETERMINATION OF THE ROBOT OPERATIONAL PARAMETERS

The operating parameters were determined for the robot arm shown in Figure 1. The analytical methods used to determine the robot operational parameters are given below.

2.1. Starting and Target Positions

Each position was determined with respect to the reference axis of the base of the frame as shown in Figures 1 and 2.

The starting position can be expressed as:

$$P_X = L_1 + L_2.C(60^o) - L_3 \quad (1)$$

$$P_Y = 50 - L_2.S(60^o) \quad (2)$$

where:

PX : Horizontal distance between the reference axis of the frame base and the terminal processor (cm)

PY : Vertical distance between the reference axis of the frame base and the terminal processor (cm)

L1, L2, and L3 : Lengths of robot arm Segments 1, 2 and 3, respectively (cm)

The target position can be expressed as:

$$P_X = L_3 + (L_2.C(\theta_2) + L_1.C(\theta_1)). + L_1.C(\theta_1) \quad (3)$$

$$P_Y = 50 + L_2.S(\theta_2) + L_1.S(\theta_1) \quad (4)$$

where:

θ_1, θ_2 : Angles of robot arm Segments 1 and 2 (degrees)

50 : Height of frame base (cm)

2.2. Orbit Planning By the Joint-Space Method

Orbital planning was performed using several polynomial equations describing the robot's motions. Third-degree or higher polynomials are often used in robot designs using the joint-space method. In this study, a third-order polynomial equation and a cubic orbit were used to represent position as a function of time. Position angles and velocities, which are related to the starting and target positions, were the main variables taken into consideration in the polynomial. Here the starting angle and target position are denoted by θ_0, θ_f, respectively, and the corresponding velocities are given by $\theta^{'} = 0, \theta^{'}(t_f) = 0$. With these conditions, the starting and target positions are not active; therefore, the velocities and angles of both of these positions were set at zero.

The third-order polynomial equation can be expressed as:

$$\theta_{(t)} = S_0 + S_1 t + S_2 t^2 + S_3 t^3 \quad (5)$$

where:

S0 : (θ0) Coefficient of starting position in the inactive condition
S1, S2, S3 : Polynomial coefficients
t : Time (seconds)

The velocities and accelerations of the robot joints were determined by taking the first and second derivatives of Equation 5, respectively.

The first derivative of Equation 5 can be expressed as:

$$\theta'_{(t)} = S_1 + 2S_2 t + 3S_3 t^2 \quad (6)$$

where:
S1, S2, S3 : Polynomial coefficients
t : Time (sec)

The polynomial coefficients can be determined from Equation 5 corresponding to specific angles of the robot. The coefficient S1 is zero in Equation 5, representing the starting time.

The polynomial coefficient S_2 can be expressed as:

$$S_2 = \frac{3}{t_{f^2}} \cdot (\theta_f - \theta_0) \quad (7)$$

where:
t_f = Time at target position (sec)
θ_f = Angle at target position (degrees)
θ_0 = Angle at starting position (degrees)

The polynomial coefficient S_3 can be expressed as:

$$S_3 = -\frac{2}{t_{f^3}} \cdot (\theta_f - \theta_0) \quad (8)$$

The robot processing time (t) between the starting and target positions in the stationary frame was taken as four seconds. The maximum joint angles corresponding to the robot shown in Figure 1 were 60º, 75º and 45º, respectively, for Joints 1, 2 and 3. Robot joint angles are inactive conditions in the starting position; therefore, the joint velocities are zero at the starting position, as shown in Figure 2. The joint positions are given at a time of 1.5 sec in the same figure. Time-position and time-velocity graphs were determined from the results of the polynomial equations, as shown in Figure 3. The maximum velocity of each joint was at t = 2 sec, and the results for the joint positions and velocities for the times of 1.5 and 2 sec, also derived from Figure 3, are given in Table 1.

The Cartesian velocities of Joint 3 were determined from the velocities of Joints 1 and 2 in a two-dimensional plane; there was a large swing velocity at t = 1.5 sec, as shown in Table 1.

Position times (sec.)		**Starting**	**Target**	**1.5 sec.**	**2 sec.**
Joint 1	Position (Degree)	0	60	18.98	30
	Velocity (Degree/sec.)	0	0	21.10	22.50
Joint 2	Position (Degree)	120	75	23.72	37.49
	Velocity (Degree/sec.)	0	0	26.36	28.12
Joint 3	Position (Degree)	60	45	14.23	22.50
	Velocity (Degree/sec.)	0	0	15.82	16.87

TABLE 1: Positions and velocities of joints at the times of 1.5 and 2 sec.

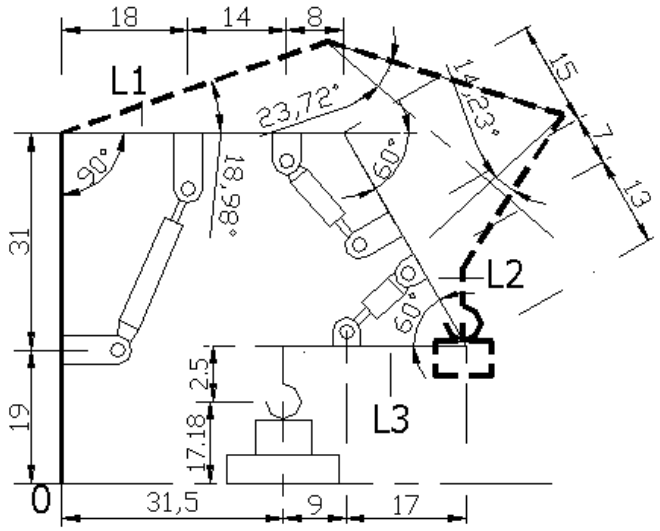

FIGURE 2: Profile view of the planar robot with three joints in the starting position and in a lifting position at a time of 1.5 sec; all dimensions are in cm

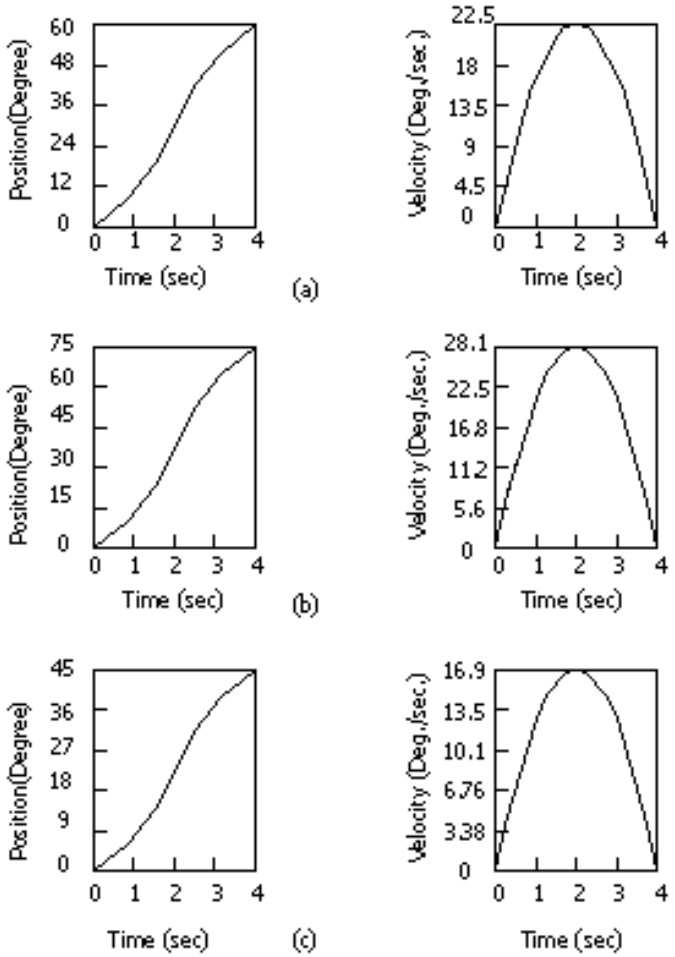

FIGURE 3: Graphs of position and velocity versus time for a) Joint 1, b) Joint 2 and c) Joint 3

The Cartesian velocities can be expressed as:

$$ {}^{0}\begin{bmatrix} V_X \\ V_Y \end{bmatrix}_3 = \begin{bmatrix} -L_1.S.\theta_1 - L_2.S\theta_{12} & -L_2.S\theta_{12} \\ L_1.C\theta_1 + L_2.C\theta_{12} & L_2.C\theta_{12} \end{bmatrix} . \begin{bmatrix} \theta_1^{'} \\ \theta_2^{'} \end{bmatrix} \quad (9) $$

where:

V_X, V_Y : Cartesian velocities of Joint 3 (m/sec)

L_1, L_2 : Lengths of robot arm Segments 1 and 2 (m)

$S\theta_{12} = S(\theta_1 + \theta_2)$: Sine representation of the joint angles in Equation 9

$C\theta_{12} = C(\theta_1 + \theta_2)$: Cosine representation of the joint angles in Equation 9

$\theta_1^{'}, \theta_2^{'}$: Joint velocities at t = 1.5 sec

The Cartesian velocities can be expressed for the robot in reverse as:

$$ {}^{0}\begin{bmatrix} V_X \\ V_Y \end{bmatrix}_3 = \begin{bmatrix} -L_3.S\theta_3 - L_2.S\theta_{32} & -L_2.S\theta_{32} \\ L_3.C\theta_3 + L_2.C\theta_{32} & L_2.C\theta_{32} \end{bmatrix} . \begin{bmatrix} \theta_3^{'} \\ \theta_2^{'} \end{bmatrix} \quad (10) $$

where:

VX, VY : Cartesian velocities of Joint 2 (m/sec)

L3, L2 : Lengths of robot arm Segments 2 and 3 (m)

$S\theta_{32} = S(\theta_3 + \theta_2)$: Sine representation of the joint angles in Equation 10

$C\theta_{32} = C(\theta_3 + \theta_2)$: Cosine representation of the joint angles in Equation 10

$\theta_3^{'}, \theta_2^{'}$: Joint velocities at t = 1.5 sec

The Cartesian velocities of the terminal processor were determined by taking the normal and reverse of the velocity matrices according to Equations 9 and 10, and the difference in the velocities of Joint 3 and Joint 2 was thus determined. Subsequently, this difference in velocities was divided by four because the mean velocities of Joints 3 and 2 and the mean velocities of the reverse kinematics give the pointedlly coordinate velocities of the terminal processor.

2.3. Robot Power Consumption

The kinetic energy of the robot arm can be expressed as [2], [8]***:***

$$ K = \frac{1}{2}\sum_{i=1}^{3} m_1.V_1^2 + \frac{1}{2}\sum_{i=1}^{3} I.\theta_a^{'\,2} \quad (11) $$

where:

K : Kinetic energy (Hp-h)

m_1, m_2, and m_3 : Masses of arm segments 1, 2 and 3 (N sec^2/m) (mass of Segment 3 (m_3) is combined with a specific load)

V_1, V_2, and V_3 : Maximum linear velocities of each arm segment (m/sec)

I_1, I_2, and I_3 : Inertial moments of each arm segment (N sec^2 m),

$\theta_a^{'}$: Angular velocities of each joint $\theta'_{a1}, \theta'_{a2}, \theta'_{a3}$ (r/sec)

The inertial moment of each arm can be expressed as [6], [8]***:***

$$ I = \frac{W}{g}.\frac{l^2}{3} \quad (12) $$

where:

W : Weight of each arm segment (the weight of the third arm segment is combined with a specific load) (N)

g : Acceleration of gravity (m/sec2)

l : Length of each arm segment (m)

The angular velocity of each joint can be expressed as [7]***:***

$$\theta'_a = \omega = \frac{V}{r} \qquad (13)$$

where:
V : Maximum linear velocity of each arm segment (m/sec)
r : Length of each arm segment; r = l (m)

The dimensions of the arm segments are given in Figure 4; the arm material is “ST 42” steel, and the arm-segment weights were computed according to the arm dimensions. The results of the arm-segment weights are given in Table 2.

Robot arm number	Weights (N)
Arm 1	105
Arm 2	37
Arm 3	27

TABLE 2: Weights of linkage arms.

First, the kinetic energy was calculated for the maximum power consumed (P) per second from Equation 11, then the kinetic-energy result was multiplied by 3,600 seconds per hour and divided by the coefficient of 75 to yield the robot power consumption [11].

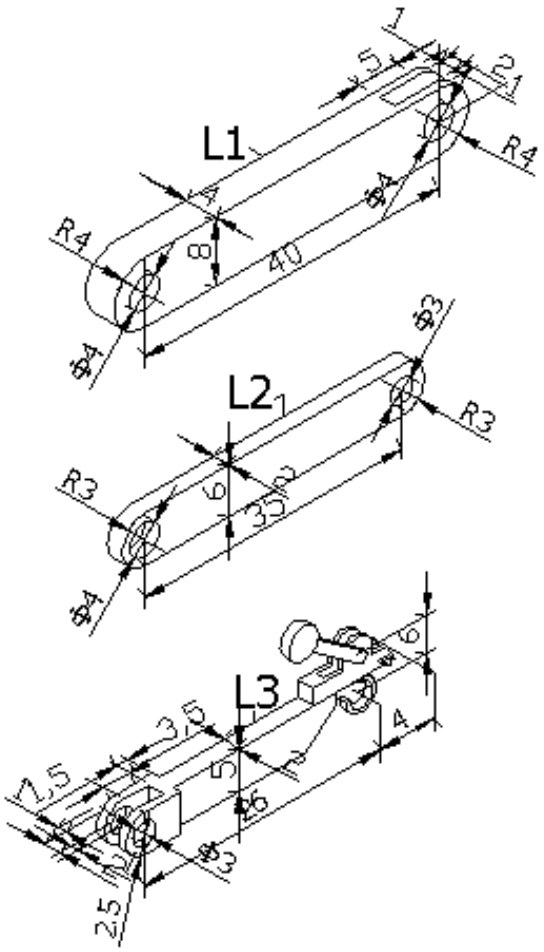

FIGURE 4: Diagrams of linkage arms and their dimensions (in cm)

3. RESULTS AND DISCUSSION

The results of the study are summarized in Table 3.

Parameters	Symbol	Results
Starting position (cm)	Px Py	31.5 17.18
Target position (cm)	Px Py	55 118.44
Maximum velocity of joints (Degree/sec.)	Joint 1 Joint 2 Joint 3	22.5 28.12 16.87
Cartesian velocity of terminal processor at 1.5 sec. (m/sec.)	Vx Vy	13.98 20.16
Cartesian velocities in reverse of terminal processor at 1.5 sec. (m/sec.)	Vx Vy	10.18 16.18
Max.linear velocities of robot arms (m/sec.)	Arm 1 Arm 2 Arm 3	0.157 0.171 0.088
Max.robot power consumtion (kW)	P	1

TABLE 3: Results of study related to the planar robot with three-joint

As evidenced by the dimensions of the positions in Table 3, the working space of the planar robot was relatively small compared to the base area, and the size of the load was small compared to the robot's weight. In these conditions, designs for the construction of larger robots with more power can be achieved via the simulation of planar robots working by hydraulic power.

The motion of the planar robots is linear and rotary in the same plane, and the terminal processor may travel a long distance because of the rotary path in the working space; therefore, the Cartesian velocities and robot power consumption are increased according to the shape of the rotary path. Another important factor causing increased power consumption is the short operational time of four seconds. Robot joint velocities were determined according to the operating time, which was taken into consideration as a basis in reaching the target position of the robot terminal processor. To this end, time-position and time-velocity graphics were determined as operational parameters (Figure 3). High velocities were determined for Joint 2 of the robot: 26.36 and 28.12 degrees/sec at the times of 1.5 and 2 seconds, respectively. The corresponding Cartesian velocities were determined as VX = -13.98 and VY = 20.16 m/sec at the time of 1.5 seconds, as shown in the Table 3. The Cartesian velocities can be considered to be at a moderate level with respect to the swing of the terminal processor with a weight of 40 N or less. In the case of a new design for a planar robot of greater dimensions and load capacity, revisions should be made to control the swing of the bigger load due to the increasing Cartesian velocities. Maximum robot power consumption was determined to be 1 kW. Generally, the power can be considered to the optimal level corresponding to a small working space. Consequently, the maximum Cartesian velocities and robot power are related to the construction dimensions and the operating time; these important parameters should thus be taken into consideration in other planar-robot designs.

4. CONCLUSION

The robot under study is considered fairly small for a large activity area and working with heavy loads. In contrast, this type of robot can be considered on the larger side for smaller areas working with a minimal activity and a light load. Designs for the construction of planar robots working on a small scale have been limited by the availability of auxiliary equipment, e.g., miniature hydraulic components, which are not generally produced in nonstandard specifications, except for the other driver unit. Generally, large constructions related to larger-scale planar robots can be designed easily and suitably for heavy industrial applications, agricultural harvesting and daily living activities. The robot in this study can be considered as

being in the middle scale of construction and at a normal level of power consumption on the basis of the scaling criteria. Consequently, the parameters resulting from this study are applicable to the design and construction of planar robots driven by hydraulic cylinders, especially in large activity areas at average operating velocities; for heavier loads, they can be chosen as initial parameters for future designs.

Nomenclature

Px Robot starting and target positions in the x direction (cm)
Py Robot starting and target positions in the y direction (cm)
υ(t) Polynomial indicator
υ'(t) Joint-velocity indicator
S2, S3 Polynomial coefficients
t Time (sec)
υf Angle of target position (degrees)
υoo Angle of starting position (degrees)
tf Time at target position (sec)
Vx Cartesian velocity in the x direction (m/sec)
Vy Cartesian velocity in the y direction (m/sec)
L1, L2 Length of robot arm Segments 1 and 2 (m)
Sυ1,2 Sine representation of the joint angles
Cυ1,2 Cosine representation of the joint angles
υ'1 , υ'2 Velocities of Joints 1 and 2 (m/sec)
K Kinetic energy (Nm)
M Mass of arm segment (N sec2/m)
V Maximum velocity of arm segment (m/sec)
I Inertial moment of arm segment (N sec2 m)
υα' Angular velocity of joint (rad/sec)
W Weight of arm segment (N)
g Acceleration of gravity (m/sec2)
r = l Length of arm segment (m)
P Maximum robot power consumption (kW)

5. REFERENCES

1. Z. Bingül and S. Kücük, "Technique of robot I" Birsen Publisher, Code No: Y.0029, İstanbul 2005.

2. A. Egrisögüt and R. Kazan, "Modelling of scara robot dynamics by using neural network" Journal of Engineer and Machine, Volume: 46 Number: 550, Ankara 2005.

3. B. Roth, "Performance evolution of manipulators from a kinematic view point" NBS, Special Publication, pp.39-61, 1975

4. Y.C. Tsa, and A.H. Soni, "Accessible region and synthesis of robot arms" ASME I., Mechanical Design, Pp.803-811, 1981.

5. C.C.D. Lin and F. Freudens Tein, "Optimization of the workspace of a three-link turning–pair connected robot arm" International Journal of Robotic Research, Vol.5, pp.104-111, 1986.

6. S. Timoshenko and D.H. Young, "Engineering Mechanic" Publisher of Civil Engineering Faculty of İTÜ. İstanbul 1975.

7. A.S. Kara, "Mechanic Problems of Engineering Analyzed" Publisher of Güven, Ankara 1974.

8. F. Yücel, “Mechanic” Publisher of Ankara Üniversity, Publisher No: 273 Course Book, No: 95, Ankara 1966.

9. N.C. Braga, “Robotic mecatronic and artificial intelligence” Publisher of Bileşim, ISBN.9752711405, İstanbul 2005.

10. S. Kücük and Z. Bingül, “Workspace optimization of fundamental robot manipulators” IEEE 12th Mediterranean Conference on Control and Automation, Kuşadası, TURKEY.2004.

11. R.A. Kepner, R. Bainer and E.I. Barger, “Principles of Farm Machinery” Third Edition Avi Publishing Company, Inc. Westport, Connecticut, 1980.